Investigation of Surface Magnetic Noise by Shallow Spins in Diamond

T. Rosskopf,[1] A. Dussaux,[1] K. Ohashi,[2] M. Loretz,[1] R. Schirhagl,[1] H. Watanabe,[3] S. Shikata,[4] K. M. Itoh,[2] and C. L. Degen[1,*]

[1]*Department of Physics, ETH Zurich, Otto Stern Weg 1, 8093 Zurich, Switzerland*

[2]*School of Fundamental Science and Technology, Keio University, Yokohama 223-8522, Japan*

[3]*Correlated Electronics Group, Electronics and Photonics Research Institute, National Institute of Advanced Industrial Science and Technology (AIST), Tsukuba Central 4, 1-1-1, Higashi, Tsukuba, Ibaraki 305-8562, Japan*

[4]*Diamond Research Group, Research Institute for Ubiquitous Energy Devices, National Institute of Advanced Industrial Science and Technology (AIST), 1-8-31, Midorigaoka, Ikeda, Osaka 563-8577, Japan*

(Received 8 November 2013; published 9 April 2014)

We present measurements of spin relaxation times (T_1, $T_{1\rho}$, T_2) on very shallow ($\lesssim$5 nm) nitrogen-vacancy centers in high-purity diamond single crystals. We find a reduction of spin relaxation times up to 30 times compared to bulk values, indicating the presence of ubiquitous magnetic impurities associated with the surface. Our measurements yield a density of 0.01–0.1μ_B/nm^2 and a characteristic correlation time of 0.28(3) ns of surface states, with little variation between samples and chemical surface terminations. A low temperature measurement further confirms that fluctuations are thermally activated. The data support the atomistic picture where impurities are associated with the top carbon layers, and not with terminating surface atoms or adsorbate molecules. The low spin density implies that the presence of a single surface impurity is sufficient to cause spin relaxation of a shallow nitrogen-vacancy center.

DOI: 10.1103/PhysRevLett.112.147602 PACS numbers: 76.30.Mi, 68.35.Dv, 75.70.Cn

Interest in the magnetic surface impurities of diamond comes from recent attempts to utilize the material for ultrasensitive, nanoscale magnetic sensor heads [1–3] and sensor arrays [4–6]. These sensors take advantage of the long-lived spin state of single nitrogen-vacancy (NV) centers to detect minute magnetic fields down to a few $\mathrm{nT}/\sqrt{\mathrm{Hz}}$ [2,7]. Diamond-based sensors have recently enabled several notable nanoscale imaging experiments, providing magnetic images of, for example, disk drive media [3,8], magnetic vortices [9], a single electron spin [10], and magnetotactic bacteria [6]. One of the most exciting prospects of diamond magnetometry is the detection and mapping of single nuclear spins under ambient conditions [1]. Such a "single-spin" nuclear magnetic resonance (NMR) microscope could have a transformative impact on structural biology and would be an extremely useful tool for the chemical analysis of surfaces. Indeed, several groups have recently reported successful detection of proton NMR from organic molecules deposited on the surface of a diamond chip [11–13] with voxels containing as few as ~300 nuclei [14].

Sensitive detection of nuclear spin signals requires placement of NV centers very close (< 10 nm) to the diamond surface. Many recent experiments, however, suggest that spin lifetimes of shallow defects are much shorter than those of bulk defects, hampering the excellent sensitivity. Enhanced magnetic noise and reduced spin lifetimes at surfaces and interfaces are well-known phenomena that have been widely studied in the context of superconducting quantum interference devices [15,16] and of donor spins in silicon [17]. A number of possible origins for this noise has been suggested, including dangling bonds [18,19], terminating surface atoms [20,21], adsorbed molecules (like paramagnetic oxygen) [22], or dynamical strain [23]. While the magnetic surface states of silicon are thought to be associated with the Si/SiO_2 interface, Bluhm *et al.* [24] recently found that a variety of surfaces are "paramagnetic," including bare Si, Au, and AlO_x. Thus, the presence of magnetic surface states seems to be common with many materials. In diamond, evidence for magnetic surface states has been found both for bulk, single crystalline surfaces [13,25,26] and for nanocrystals [20,21,27–29]. Electron paramagnetic resonance and optically detected magnetic resonance have been used to indirectly estimate a density $\rho_A = 0.1\text{–}10\mu_B/\mathrm{nm}^2$ and characteristic correlation time $\tau_c = 10^{-11}\text{–}10^{-5}$ s of surface magnetic states [21,29,30], but reported values are not consistent. The goal of this study is to provide a quantitative picture of ρ_A and τ_c, so as to more precisely pinpoint the atomistic origin of the surface noise.

Presented here are spin relaxation time measurements for a series of shallow ($\lesssim$5 nm) NV centers in high-purity, single crystalline diamond. Spin relaxometry is widely used in the fields of NMR and electron paramagnetic resonance to investigate dynamic (ps-μs) processes in materials [15,17,31]. The method relies on the fact that the spin flip rate r is proportional to the magnetic noise spectral density $S_B(\omega)$ evaluated at the transition frequency ω (Fermi's golden rule). In this study, we exploit multiple relaxation times, including T_1, $T_{1\rho}$, and T_2, to probe the noise spectral

 © 2014 American Physical Society

density over a wide frequency range. This method allows us to directly and quantitatively derive τ_c and ρ_A. We have applied our technique to a series of NV centers exposed to different surface terminations, atmospheres, and temperatures.

The principal relaxation times used in this study are the spin-lattice relaxation time T_1 and the rotating-frame relaxation time $T_{1\rho}$ that probe $S_B(\omega)$ in the $\omega \sim$ GHz and $\omega \sim$ MHz regimes, respectively. Figures 1(a) and 1(b) identify the transition rates relevant for these relaxation times. r_0 is the rate of spin flips between the $|0\rangle$ and the (nearly degenerate) $|\pm 1\rangle$ states over an energy gap of $\omega_0 \approx 2\pi \times 2.87$ GHz given by the zero-field splitting [34]. r_1 is the rate of spin flips between parallel and antiparallel states in a spin-locking experiment [35] with a smaller energy gap given by the Rabi frequency ω_1 (typically $\omega_1 \approx 2\pi \times 10$ MHz). The relaxation times T_1 and $T_{1\rho}$ associated with r_0 and r_1 are [36]

$$T_1^{-1} = 6r_0 = \frac{\gamma^2}{2} S_B(\omega_0), \tag{1}$$

$$T_{1\rho}^{-1} \approx 2r_1 + 3r_0 = \frac{\gamma^2}{6} S_B(\omega_1) + \frac{\gamma^2}{4} S_B(\omega_0), \tag{2}$$

where $S_B = S_{B_x} + S_{B_y} + S_{B_z}$ is the sum of the three components of the (double-sided) magnetic noise spectral density [37] and where we have assumed that

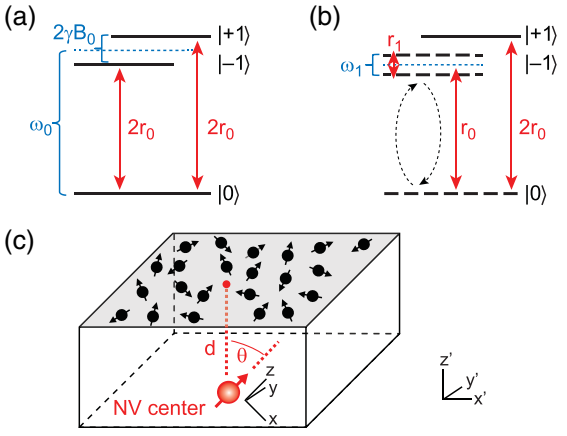

FIG. 1 (color online). (a),(b) Energy level diagram of the NV center's spin $S = 1$ system, indicating allowed spin transitions (red solid arrows) and associated transition rates r_0 and r_1. Blue brackets indicate the energy gaps between states. ω_0 is the Larmor frequency (~2.9 GHz) and ω_1 is the Rabi frequency (~10 MHz). A small bias field ($B_0 \sim 10$ mT) lifts the degeneracy between $|\pm 1\rangle$ [32,33]. Diagram (a) shows transitions relevant for the T_1 measurement and diagram (b) shows transitions relevant for the $T_{1\rho}$ measurement. Dashed levels and arrows in (b) symbolize the superposition between $|0\rangle$ and $|-1\rangle$. (c) Basic picture of diamond surface magnetic impurities. Surface states are represented by a two-dimensional bath of electron spins that produce a fluctuating magnetic field. A nearby shallow NV center is used as a local probe to pick up the magnetic noise and analyze the spectral characteristics.

$S_B(\omega_1) \gtrsim S_B(\omega_0)$ and $B_0 \ll D$ (see Fig. 1). The magnetic noise spectral density expressed as a function of measured T_1 and $T_{1\rho}$ is

$$S_B(\omega_0) = \frac{2}{\gamma^2 T_1}, \tag{3}$$

$$S_B(\omega_1) = \frac{6}{\gamma^2 T_{1\rho}} - \frac{3}{2} S_B(\omega_0). \tag{4}$$

We will interpret the magnetic noise in terms of a two-dimensional bath of electron spins ($S = 1/2$) located at a distance d from the NV center, illustrated in Fig. 1(c). The two-dimensional bath produces a cumulative magnetic field given by the sum of (randomly oriented) magnetic dipoles:

$$B_{\mathrm{rms}}^2 = \left(\frac{\mu_0}{4\pi}\right)^2 \iint_{-\infty}^{+\infty} dx'dy' \frac{\rho_A}{r'^6} \sum_{k=x,y,z} \left| \frac{3\mathbf{r}'(\mathbf{m}_k \cdot \mathbf{r}')}{r'^2} - \mathbf{m}_k \right|^2, \tag{5}$$

where ρ_A is the uniform areal density of surface dipoles, $\mathbf{r}' = (x', y', d)$ is the spatial position (with the NV center located at the origin), $r' = |\mathbf{r}'|$, $\mathbf{m}_k$ are the three components of a surface dipole, and $|\mathbf{m}_k| = \hbar\gamma/2$. For a (100)-oriented surface the NV spin is at $\theta \approx 54.7°$ to the surface normal, and evaluation of the integral yields [36]

$$B_{\mathrm{rms}}^2 = \frac{3\mu_0^2 \hbar^2 \gamma_S^2}{64\pi} \frac{\rho_A}{d^4} \approx (2.85\ \mathrm{mT\,nm^3})^2 \frac{\rho_A}{d^4}. \tag{6}$$

Provided that the depth d of an NV center is known one may use Eq. (7) to infer the density of surface states:

$$\rho_A \approx \frac{B_{\mathrm{rms}}^2 d^4}{(2.85\ \mathrm{mT\,nm^3})^2}. \tag{7}$$

The magnetic field B_{rms} is not static but fluctuates according to the dynamics of the spin bath. In general, these dynamics may be complex and may involve multiple time constants. In spite of this we will interpret dynamics by a single autocorrelation time τ_c. We will find below that this approach produces consistent results, but fails to capture the low-frequency noise introduced by intrinsic donor spins. The advantage of describing dynamics by a single autocorrelation time τ_c is that quantitative values for τ_c and B_{rms} can be directly inferred from a single pair of relaxation times, providing an efficient means for analyzing many experimental conditions [38]. The magnetic noise spectral density associated with τ_c is

$$S_B(\omega) = B_{\mathrm{rms}}^2 \frac{\tau_c^{-1}}{\omega^2 + \tau_c^{-2}}. \tag{8}$$

From Eq. (8) τ_c and B_{rms} are directly inferred as

$$\tau_c^{-2} = \frac{R\omega_0^2 - \omega_1^2}{1 - R}, \tag{9}$$

$$B_{\mathrm{rms}}^2 = S_B(\omega_0)\frac{\omega_0^2 + \tau_c^{-2}}{\tau_c^{-1}}, \tag{10}$$

where $R = S_B(\omega_0)/S_B(\omega_1) = r_0/r_1 \ll 1$.

We have measured spin relaxation times for a series of shallow ($\lesssim 5$ nm) NV centers in two different single crystalline samples. These samples had originally been prepared for other experiments [13,25], and the data presented here were partially acquired during these measurements. Sample A was a 17-nm-thin film of ^{13}C-depleted diamond grown on top of a bulk crystal by chemical vapor deposition [13,35,39]. The topmost 5 nm of this film were doped with nitrogen (~10 ppm) during growth, and only this film was found to host NV centers [13]. Sample B was an electronic-grade single crystal grown by chemical vapor deposition that was scaife polished, nitrogen implanted at low energy (0.4–5 keV) and annealed, resulting in NV centers at roughly 1–10 nm from the surface [25]. Both samples had a (100) surface orientation. Sample A was further investigated under three different surface chemistries, including hydrogen, oxygen, and fluorine terminations. Sample B was only investigated under oxygen termination. More details on sample growth and surface preparation are given with Refs. [13,25].

Spin relaxation times were measured by optically detected magnetic resonance spectroscopy at room temperature and on single NV centers [40]. Protocols are explained in Fig. 2: For T_1 measurements, the spin was prepared in the $|0\rangle$ state by a first laser pulse and the final state measured by a second laser pulse based on the NV center's spin-dependent luminescence [40]. Pump and probe pulses were separated by a dark interval of duration τ during which relaxation occurred. Two decay curves were recorded for each NV center with the spin state initialized in the $|0\rangle$ and $|1\rangle$ states, respectively. The curves were then subtracted and the differential probability Δp [36] fit to the exponential function given with Fig. 2. This technique gives a simple exponential decay with a zero baseline and a single decay constant that fits more robustly than the

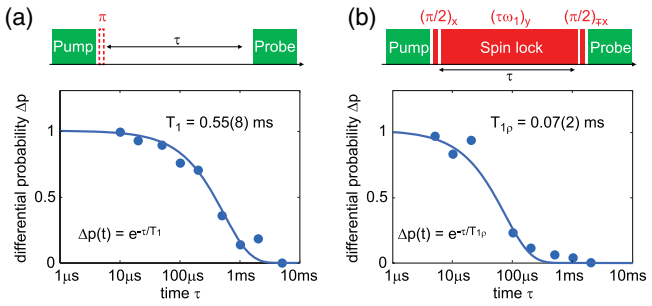

FIG. 2 (color online). Pulse-timing diagrams and example decay curves for measurements of (a) the spin-lattice relaxation time T_1 and (b) the rotating-frame relaxation time $T_{1\rho}$. Green "pump/probe" blocks symbolize laser pulses (~1 μs) and red other blocks symbolize microwave pulses. Red dotted block and "$\pm x$" denote phase cycling for the differential measurement. Curves are exponential fits and dots represent experimental values. Data shown is for NV No. 8 in Fig. 3 measured on sample A.

individual decay curves [32,36]. For $T_{1\rho}$ measurements, three microwave pulses were used to create a "spin lock" situation [35] [see Fig. 2(b)]. Again, two decay curves were recorded and subtracted using phase cycling of the second $\pi/2$ microwave pulse.

Figure 3 collects and analyzes measurements obtained from 13 different NV centers. In a first panel [Fig. 3(a)] we plot $T_{1\rho}$ as a function of T_1. This plot serves to illustrate two findings: To begin, we observe that relaxation times are reduced up to 30 times compared to bulk values [here $T_1^{\mathrm{bulk}} = 12(2)$ ms for sample A and $T_1^{\mathrm{bulk}} = 4.5(2)$ ms for sample B]. This shows that surface effects are indeed present and that both T_1 and $T_{1\rho}$ are sensitive indicators of surface magnetic noise. The baseline noise, taken as $S_B^{\mathrm{bulk}}(\omega_0) = 2/(\gamma^2 T_1^{\mathrm{bulk}})$, is only 73 pT/Hz$^{1/2}$ for sample A, illustrating the sensitivity of the measurement. Second, we observe that $T_{1\rho}$ and T_1 are strongly correlated. NV centers with long T_1 times also have long $T_{1\rho}$, and NV centers with short T_1 times also exhibit short $T_{1\rho}$. The ratio between T_1 and $T_{1\rho}$ is fairly consistent at about 10:1.

Figure 3(a) additionally plots values of the spin echo decay time T_2. We note that T_2 is not correlated with T_1. Thus, T_2 relaxation is governed by low-frequency (~kHz) noise that is not related to the surface, such as the noise produced by nitrogen donors within diamond.

Figures 3(b) and 3(c) plot values of the characteristic correlation time τ_c and the rms magnetic field B_{rms} organized by surface chemistry and sample type. [Note that the baseline noise $S_B^{\mathrm{bulk}}(\omega_0)$ was subtracted from both $S_B(\omega_0)$ and $S_B(\omega_1)$ to account for surface-unrelated or "bulk" relaxation.] We find that τ_c shows little variation with almost all values between 0.2 and 0.4 ns. This finding is surprising, because a strong variation of τ_c would be expected if magnetic surface states were rooted in terminating surface atoms or adsorbates. Much larger variations are found for B_{rms}, as can be expected from the stochastic placement of NV centers and surface impurities.

In Fig. 3(d) we have calculated the surface spin density ρ_A according to Eq. (7). Although we do not have a precise knowledge of the depth d of individual NV centers, we know that $d \lesssim 5$ nm given the 5-nm-thick doping layer of the sample (sample A) [41]. For sample B the depth was estimated through stopping range of ions in matter calculations [25]. Among the NV centers of sample A we have picked the ones with the lowest B_{rms} for each surface termination (here ~20 μT) and assumed a depth of $d = 5$ nm. This yields an upper bound for ρ_A. In fact, since many NV centers showed similar $B_{\mathrm{rms}} \sim 20$ μT, we suspect that most NV centers are located near the deep end of the doping layer. We find that $\rho_A = 0.01$–$0.1\mu_B/\mathrm{nm}^2$ (upper bound) for both samples [see Fig. 3(d)]. The lowest densities are observed for fluorine-terminated surfaces and the highest densities for the implanted surface, respectively.

The densities of surface impurities found here are low compared to previous results from nanodiamonds [20,29] and from superconducting quantum interference device measurements on other material surfaces [24], where

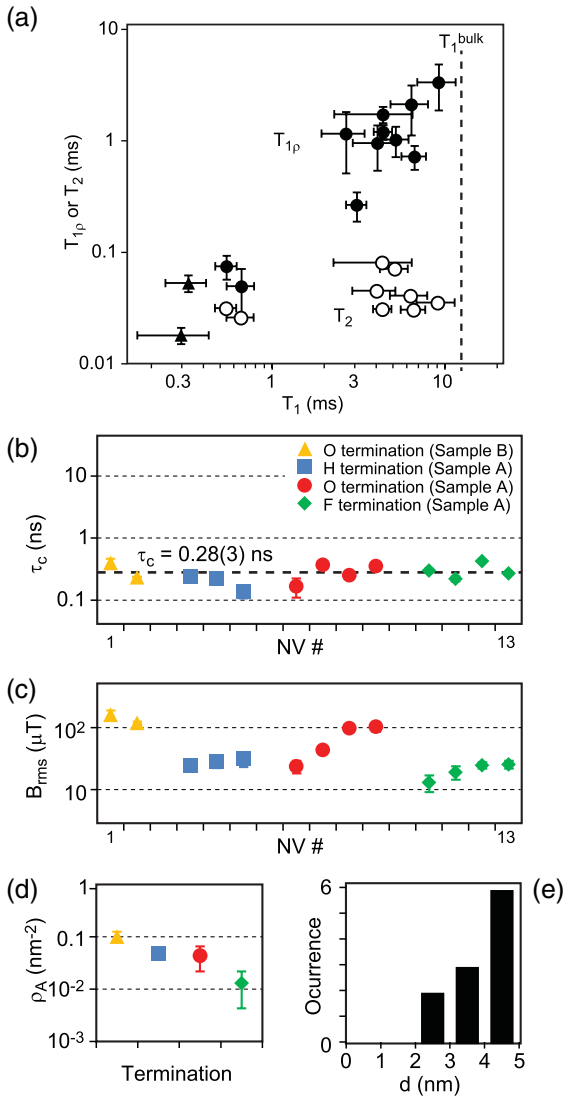

FIG. 3 (color online). Spin relaxation time measurements of 13 shallow NV centers for different samples and surface terminations. (a) T_1, $T_{1\rho}$, and T_2 times organized in a two-dimensional correlation plot. Observed relaxation times are $T_1 = 0.3$–9 ms, $T_{1\rho} = 0.02$–3 ms, and $T_2 = 22$–80 μs. Dots represent sample A and triangles represent sample B. Bulk $T_1^{\text{bulk}} = 12(2)$ ms (sample A) is indicated by a dashed line. (b) Autocorrelation time τ_c of surface fluctuations for the same NV centers, organized by sample and surface termination. (c) rms magnetic field B_{rms} for each NV center. (d) Density of surface impurities ρ_A for samples and surface terminations. (e) Histogram of depth values (upper bound) of NV centers inferred from B_{rms}. Errors are propagated from fits to T_1 and $T_{1\rho}$ decay curves. Numerical data are provided as Supplemental Material [36].

$\rho_A \sim 1$–$10\mu_B/\text{nm}^2$. We believe that this is a consequence of the high surface quality of the present samples. Given the low density and close proximity of investigated NV centers to the surface, we expect that only very few surface states show significant coupling to the NV spin. In fact, we have calculated that at a depth of $d \sim 3$ nm about 80% of B_{rms}^2 will, on average, originate from a single surface impurity. This means that at shallow depths a single impurity is responsible for spin relaxation. While this is an exciting prospect in the context of quantum sensing [10,42], it is difficult to confirm and utilize the "quantum" character of these surface states due to the short τ_c.

Our data also give insight into the mechanism causing fluctuations. Two main mechanisms have been suggested including spin diffusion and spin-phonon relaxation [15,29]. The low density ρ_A of surface states in our samples favors spin-phonon relaxation over spin diffusion. This hypothesis is supported by the observation that all investigated surfaces show similar correlation times τ_c irrespective of ρ_A.

To more conclusively establish the mechanism of noise generation we have recorded T_1 of one NV center as a function of temperature. Since $\tau_c \propto T_1$ according to Eq. (8) a temperature dependence of T_1 directly indicates whether fluctuations are thermally activated, as predicted for a spin-phonon (but not a spin diffusion) process [32]. As Fig. 4(a) shows, T_1 is strongly temperature dependent, indicating that surface fluctuations are indeed thermally activated.

We finally discuss a few anecdotal observations. In an attempt to perform nanoscale NMR measurements with shallow NV centers [11–13] we have over coated the diamond surface with a variety of substances and recorded the associated relaxation times. We did not find any significant changes with any of the substances tested, including stearic acid and optical immersion oils (data not shown). We have finally exposed the sample to vacuum, ambient air, and 100% oxygen atmospheres, with no noticeable change in T_1 [see Fig. 4(b)]. We can thus exclude molecular oxygen as the leading cause of surface magnetic noise. Together, all observations support the general picture where the surface states are intrinsically associated with diamond's top carbon layers [19] and not with terminating surface atoms or adsorbate molecules.

In the light of these findings, several illuminating experiments could be conceived. In particular, different surface orientations of diamond [such as a (111)-oriented surface] or atomically flat substrates [43] could be explored to elucidate the influence of bonding structure of the top carbon atoms. Altogether, a precise understanding of

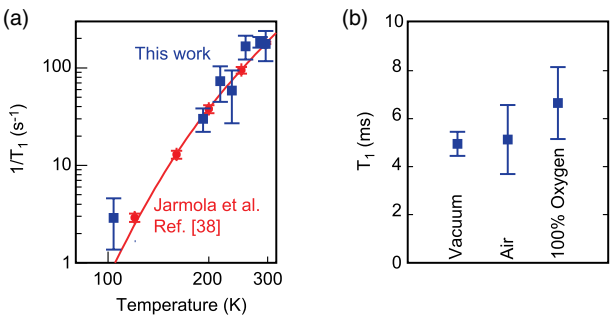

FIG. 4 (color online). (a) Temperature dependence of T_1 for a shallow NV center (Sample A, red dots) and for bulk NV centers (from Ref. [32], Fig. 2, curve S8). (b) T_1 for the same NV center, showing no significant change in T_1 with exposure to different oxygen pressures.

diamond surface magnetic states will be crucial for further improving the sensitivity and resolution of diamond magnetic sensor heads and sensor arrays.

The work at ETH was supported by the Swiss National Science Foundation through Project Grant No. 200021_137520/1 and through the NCCR QSIT. The work at Keio has been supported by the Cannon Foundation, the Core-to-Core Program by JSPS, and the Project for Developing Innovation Systems by MEXT. We thank K. Chang and F. Jelezko for experimental help and fruitful discussions, and J. Meijer and S. Pezzanga for help with the preparation of sample *B* [25].

*degenc@ethz.ch

[1] C. L. Degen, Appl. Phys. Lett. **92**, 243111 (2008).
[2] G. Balasubramanian *et al.*, Nature (London) **455**, 648 (2008).
[3] P. Maletinsky, S. Hong, M. S. Grinolds, B. Hausmann, M. D. Lukin, R. L. Walsworth, M. Loncar, and A. Yacoby, Nat. Nanotechnol. **7**, 320 (2012).
[4] D. M. Toyli, C. D. Weis, G. D. Fuchs, T. Schenkel, and D. D. Awschalom, Nano Lett. **10**, 3168 (2010).
[5] S. Steinert, F. Dolde, P. Neumann, A. Aird, B. Naydenov, G. Balasubramanian, F. Jelezko, and J. Wrachtrup, Rev. Sci. Instrum. **81**, 043705 (2010).
[6] D. Le Sage, K. Arai, D. R. Glenn, S. J. DeVience, L. M. Pham, L. Rahn-Lee, M. D. Lukin, A. Yacoby, A. Komeili, and R. L. Walsworth, Nature (London) **496**, 486 (2013).
[7] J. R. Maze *et al.*, Nature (London) **455**, 644 (2008).
[8] L. Rondin, J.-P. Tetienne, P. Spinicelli, C. Dal Savio, K. Karrai, G. Dantelle, A. Thiaville, S. Rohart, J.-F. Roch, and V. Jacques, Appl. Phys. Lett. **100**, 153118 (2012).
[9] L. Rondin, J.-P. Tetienne, S. Rohart, A. Thiaville, T. Hingant, P. Spinicelli, J.-F. Roch, and V. Jacques, Nat. Commun. **4**, 2279 (2013).
[10] M. S. Grinolds, S. Hong, P. Maletinsky, L. Luan, M. D. Lukin, R. L. Walsworth, and A. Yacoby, Nat. Phys. **9**, 215 (2013).
[11] H. J. Mamin, M. Kim, M. H. Sherwood, C. T. Rettner, K. Ohno, D. D. Awschalom, and D. Rugar, Science **339**, 557 (2013).
[12] T. Staudacher, F. Shi, S. Pezzagna, J. Meijer, J. Du, C. A. Meriles, F. Reinhard, and J. Wrachtrup, Science **339**, 561 (2013).
[13] K. Ohashi *et al.*, Nano Lett. **13**, 4733 (2013).
[14] M. Loretz, S. Pezzagna, J. Meijer, and C. L. Degen, Appl. Phys. Lett. **104**, 033102 (2014).
[15] R. de Sousa, Phys. Rev. B **76**, 245306 (2007).
[16] F. C. Wellstood, C. Urbina, and J. Clarke, Appl. Phys. Lett. **50**, 772 (1987).
[17] T. Schenkel, J. A. Liddle, A. Persaud, A. M. Tyryshkin, S. A. Lyon, R. de Sousa, K. B. Whaley, J. Bokor, J. Shangkuan, and I. Chakarov, Appl. Phys. Lett. **88**, 112101 (2006).
[18] V. Y. Osipov, A. Shames, and A. Y. Vul', Physica (Amsterdam) **404B**, 4522 (2009).
[19] N. D. Samsonenko, G. V. Zhmykhov, V. S. Zon, and V. K. Aksenov, J. Struct. Chem. **20**, 951 (1980).
[20] J. Tisler *et al.*, ACS Nano **3**, 1959 (2009).
[21] L. P. McGuinness *et al.*, New J. Phys. **15**, 073042 (2013).
[22] R. C. Bansal, F. J. Vastola, and P. L. Walker, Carbon **10**, 443 (1972).
[23] J. M. Moore, and M. E. Flatté, in *Proceedings of the APS March Meeting* (Baltimore, 2013) (Report No. B46.00014).
[24] H. Bluhm, J. A. Bert, N. C. Koshnick, M. E. Huber, and K. A. Moler, Phys. Rev. Lett. **103**, 026805 (2009).
[25] B. K. Ofori-Okai, S. Pezzagna, K. Chang, M. Loretz, R. Schirhagl, Y. Tao, B. A. Moores, K. Groot-Berning, J. Meijer, and C. L. Degen, Phys. Rev. B **86**, 081406 (2012).
[26] K. Ohno, F. Joseph Heremans, L. C. Bassett, B. A. Myers, D. M. Toyli, A. C. Bleszynski Jayich, C. J. Palmstrom, and D. D. Awschalom, Appl. Phys. Lett. **101**, 082413 (2012).
[27] A. Laraoui, J. S. Hodges, and C. A. Meriles, Nano Lett. **12**, 3477 (2012).
[28] A. M. Panich, A. I. Shames, H.-M. Vieth, E. Ōsawa, M. Takahashi, and A. Ya. Vul', Eur. Phys. J. B **52**, 397 (2006).
[29] J. P. Tetienne, T. Hingant, L. Rondin, A. Cavaillès, L. Mayer, G. Dantelle, T. Gacoin, J. Wrachtrup, J.-F. Roch, and V. Jacques, Phys. Rev. B **87**, 235436 (2013).
[30] H. J. Mamin, M. H. Sherwood, and D. Rugar, Phys. Rev. B **86**, 195422 (2012).
[31] R. Kimmich, and E. Anoardo, Prog. Nucl. Magn. Reson. Spectrosc. **44**, 257 (2004).
[32] A. Jarmola, V. M. Acosta, K. Jensen, S. Chemerisov, and D. Budker, Phys. Rev. Lett. **108**, 197601 (2012).
[33] A small bias field does not significantly alter the relaxation dynamics; the error added to spectral densities is $< 2\%$.
[34] M. W. Doherty, N. B. Manson, P. Delaney, F. Jelezko, J. Wrachtrup, and L. C. L. Hollenberg, Phys. Rep. **528**, 1 (2013).
[35] M. Loretz, T. Rosskopf, and C. L. Degen, Phys. Rev. Lett. **110**, 017602 (2013).
[36] See Supplemental Material at http://link.aps.org/supplemental/10.1103/PhysRevLett.112.147602 for derivations, fit functions, and additional datasets.
[37] The magnetic field is isotropic assuming that surface spins are randomly oriented and the NV center's spin is at an angle of $\theta = 54.7°$ from the surface normal (see Supplemental Material [36]).
[38] We note that while the entire noise spectral density could, in principle, be mapped out by field cycling [31], these measurements are impractical due to the long acquisition times involved and yield ambiguous results due to the field dependence of surface spin dynamics.
[39] T. Ishikawa, K.-M. C. Fu, C. Santori, V. M. Acosta, R. G. Beausoleil, H. Watanabe, S. Shikata, and K. M. Itoh, Nano Lett. **12**, 2083 (2012).
[40] A. Gruber, A. Dräbenstedt, C. Tietz, L. Fleury, J. Wrachtrup, C. von Borczyskowski, Science **276**, 2012 (1997).
[41] The thickness of the δ-doped layer was estimated from the calibrated growth rate and is expected to be accurate within 20%. See also Refs. [13,39].
[42] M. Schaffry, E. M. Gauger, J. J. L. Morton, and S. C. Benjamin, Phys. Rev. Lett. **107**, 207210 (2011).
[43] H. Watanabe, D. Takeuchi, S. Yamanaka, H. Okushi, K. Kajimura, and T. Sekiguchi, Diam. Relat. Mater. **8**, 1272 (1999).